

NEDLA TEST SITE REPORT

Sikhote-Alin Site

Tatiana Loboda ¹, Guoqing Sun ^{1,2}, Zhiyu Zhang ¹

¹ University of Maryland, Geography Department

² NASA Goddard Space Flight Center

Contents

1	Site Location	2
1.1	Country, State, Province	2
1.2	Center coordinates	2
1.3	Geographic settings and environmental characteristics	2
1.4	Major types of vegetation disturbance and land cover change	3
2	Satellite Imagery	3
3	Auxiliary data	3
4	Mapping Legend	3
5	Land Cover Map	6
5.1	Pre-processing	6
5.2	Land cover classification	7
5.2.1	Masks	7
5.2.2	Development of metrics for image classification	7
5.2.3	Mapping vegetation classes	7
5.3	Post-classification processing	8
5.4	Accuracy assessment	8
5.4.1	Aggregated classes accuracy assessment	8
5.4.2	Full classification accuracy assessment	9
5.5	Analysis of mapping results	11
5.6	Comparison to coarse resolution land cover maps	12
6	Land Cover Change Map	14
6.1	Pre-processing	14
6.1.1	Mature forest mapping	14
6.1.2	Accuracy assessment for mature forest mapping	14
6.2	Change detection	15
6.3	Post-classification processing	16
6.4	Accuracy assessment	16
6.5	Results of the land cover change map	16
6.6	Analysis of the land cover change map	18
7	Publications Using the Site Data	20
8	List of Contributors to Site Data and Report	20
9	Acknowledgements	20
10	References	20

1 Site Location

1.1 Country, State, Province

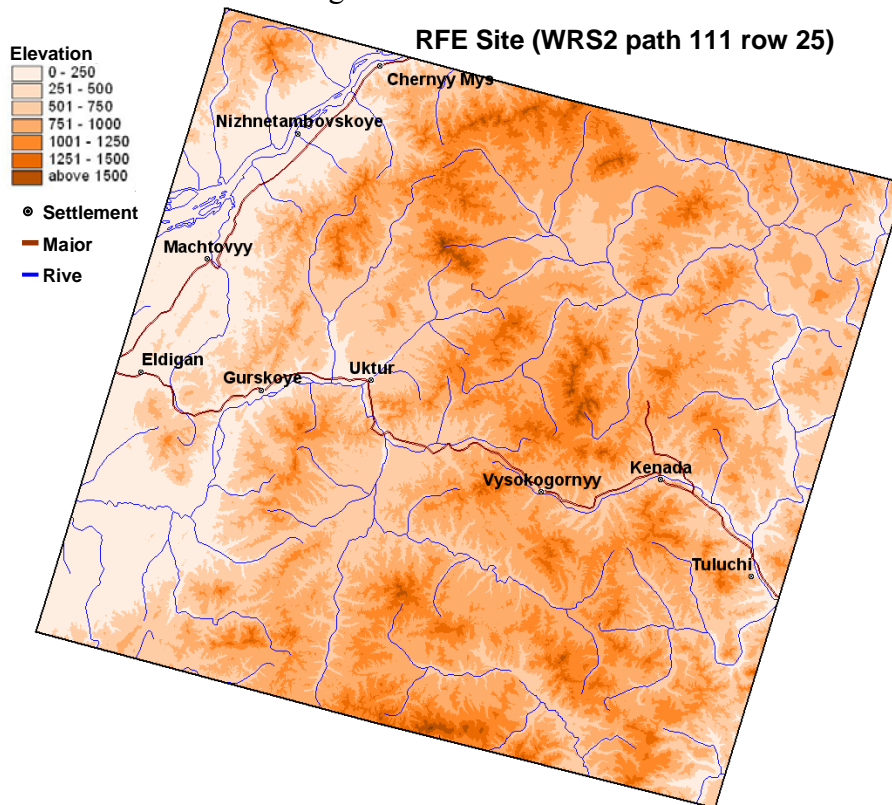
The test site is located in the northern part of the Sikhote-Alin Mountain range and the south-eastern part of Khabarovsk Krai of the Russian Federation.

1.2 Center coordinates

50.3° N, 138.9° E (Landsat WRS2 path 111 row 25)

1.3 Geographic settings and environmental characteristics

The site is located in a transition zone between middle taiga and temperate forests of the northern Sikhote-Alin Mountains. The site stretches between the Amur river in the west as it turns north-east and away from the border between Russia and China and the Tatar Strait of the Sea of Japan in the east. Elevations range between 200 and 2000m with the mean elevation around 600m.



Although found below 50° N ecosystems within this site developed in cold alpine conditions due to presence of the Sikhote-Alin Mountain range with mean annual temperatures ranging between -5 to 0 °C (Stolbovoi and McCallum, 2002). Only flat areas in the western part of the site along the Amur River have mean annual temperatures between 0 and 5°C. Although this area is immediately adjacent to the Sea of Japan and should

experience the influence of the warm Kuroshio current in the west Pacific, the dominance of the Siberian High during winter months amplified by the altitudinal gradient supports mean January temperatures between -20 °C at lower elevations and -25 °C at higher elevations. Mean July temperatures vary considerably between the lower elevations (19 – 21 °C) and higher elevations (10-12 °C). The area receives abundant amount of precipitation (500-700 mm) brought in by the summer monsoon with increased precipitation rate driven by the topographic barrier established by the Sikhote-Alin mountains. This is one of few regions in Northern Asia where permafrost is absent everywhere except at the highest elevations.

The site has one of the highest total phytomass densities in Russia (on average above 7 km/m² with some areas above 12.6 km/m²) (Stolbovoi and McCallum, 2002). The majority of phytomass is contained in the above ground layer (up to 4 times as much as above ground). Larch and spruce-fir forest are dominant communities. However, oak, birch and aspen are also found throughout the area. The region is generally a biodiversity hotspot including such highly endangered species as the Amur Tiger.

The majority of the area is within commercial forestry land use with small sections used for crop production and rangelands.

1.4 Major types of vegetation disturbance and land cover change

Timber harvesting presents the major type of anthropogenic disturbance. Natural disturbances are represented by wildland fire and insect infestation. The oak forests are susceptible to damage from the green Oak-roller moth while pine forests affected by the nun moth (both with average infestation rates between 6 and 25 %) (Stolbovoi and McCallum, 2002). Wildland fires, although not as frequent as in other regions of Northern Eurasia, strongly modify land cover of the Sikhote-Alin. The study site is within the zone of highest contiguous extent of burned areas on the landscape with up to 6.7 % of total area burned.

2 Satellite Imagery

Landsat TM, and ETM+ (WRS2 p111 r25) images present the primary source of data for land cover mapping and change detection. The image stack includes 3 images and covers the time period between 1990 and 2005.








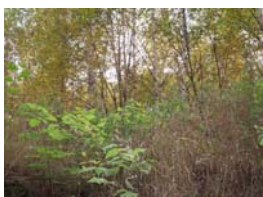
Instrument	Acquisition date	Use	Notes
Landsat TM	08/13/1990	primary	change detection basis
Landsat ETM+	05/18/2002	primary	classification basis, change detection basis
Landsat TM	09/07/2005	primary	change detection basis








3 Auxiliary data

QuickBird images available at GoogleEarth were visually examined to identify urban areas and in defining training and validation pixels for the classification. In addition, the Shuttle Radar Topography Missions (SRTM) dataset was used to apply topographic correction to image data values. A limited sample of vegetation measurements were collected during field campaign in September of 2006. These locations were used to train the analyst to identify land cover types (and particularly differentiate between Tree.needleleaf.evergreen. and Tree.needleleaf.deciduous classes) in high resolution imagery within Google Earth.

4 Mapping Legend

The following land cover classes consistent with the NELDA Land Cover Legend were identified within the scene.

<i>Class ID</i>	<i>Description</i>	<i>Examples</i>
1	Tree.needleleaf.evergreen.closed	
2	Tree.needleleaf. evergreen.open	
3	Tree.needleleaf.deciduous.closed	
4	Tree.needleleaf.deciduous.open	
5	Tree.mixed.closed	
6	Tree.mixed.open	
7	Tree.broadleaf.deciduous.closed	
8	Tree.broadleaf.deciduous.open	

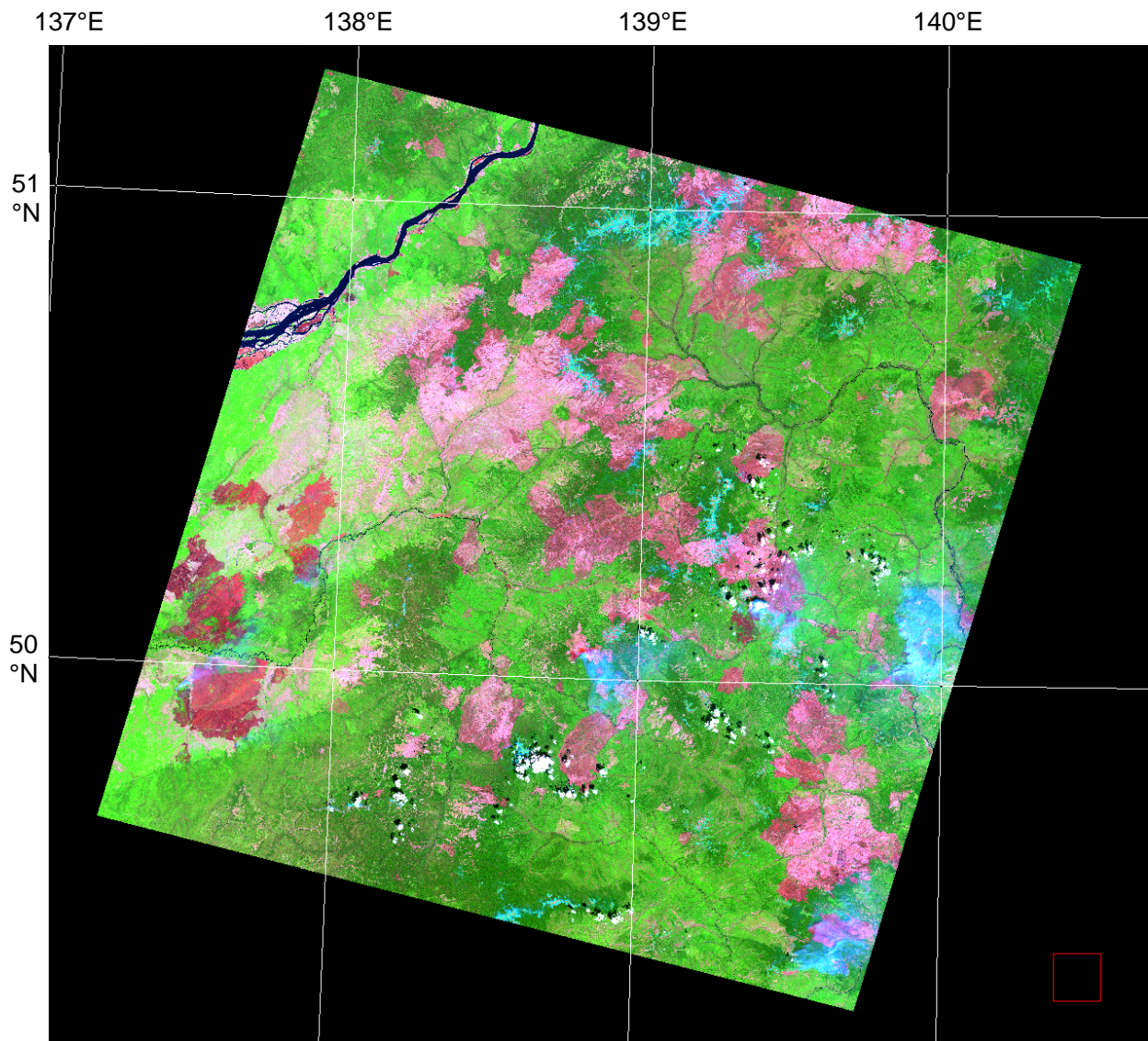
9	Tree.mixed.open.mortality	
10	Shrub.mixed.closed	
11	Shrub.mixed.open	
12	Herbaceous	
13	Bare.sparse	
14	Bare.built	
15	Water	
16	Cloud/Shadow	

5 Land Cover Map

5.1 Pre-processing

The main classification image was orthorectified as part of the Tri-decadal Landsat Orthorectified archive (http://eros.usgs.gov/products/satellite/landsat_ortho.php). Further image pre-processing involved performing terrain correction using the SRTM DEM data obtained from the Global Land Cover Facility (<http://glcf.umd.edu/index.shtml>) following the methodology for the sun-canopy-sensor topographic correction in forested terrain (Soenen et al., 2005). The topographic correction was performed on the digital numbers which were subsequently converted to at sensor reflectance and atmospherically corrected using the COST method (Chavez, 1996).

Landsat/ETM+ image from 05/18/2002



5.2 Land cover classification

5.2.1 Masks

Several masks developed prior to classifying the image to eliminate potential confusion of classes:

- i) background mask – areas of the image which contain no valid data values
- ii) water mask – thresholded in NIR and hand digitized
- iii) fresh burns were mapped using supervised Spectral Angle Mapping approach and MODIS active fire detections (see specific description of the approach in Loboda et al., 2007)
- iv) “bare” ground mask – thresholded in NDVI and tasseled cap surface brightness with clouds and smoke-affected areas manually removed from the class
- v) “built up” mask was manually selected from the “bare” mask following point shapefile distribution of settlements obtained from the Digital Chart of the World (<<http://www.maproom.psu.edu/dcw/>>) and Google Earth high resolution imagery
- vi) “bare.sparse” class was identified as remaining after the removal of “bare.built” from “bare ground” identified in step iv.

5.2.2 Development of metrics for image classification

Additional metrics were calculated to support decision tree application:

- i) Normalized Burn Ratio (NBR)
- ii) NDVI
- iii) Principal Components
- iv) Tasseled Cap (using surface reflectance indices published in Crist, 1985)

These metrics and the original 7 bands (including resampled thermal band) were stacked in one file.

5.2.3 Mapping vegetation classes

- i) Training samples for visually identifiable in high resolution (Quickbird available at Google Earth) and the classification image from 5/18/2002 were selected across the classification scene.
- ii) Training spectra for each class from the full stack of classification metrics were extracted and reformatted for further processing in the statistical software
- iii) S-Plus statistical package was used to develop a decision tree algorithm
- iv) the decision tree rules were implemented within the “vegetative cover” mask developed after exclusion of background, water, and previous burns.

5.2.4 Mapping vegetation in smoke affected areas

Large sections of the classified image (~5-10%) were affected by smoke plumes from on-going wildland fires. These areas were masked out from the original classification and reclassified using analyst-selected training pixels found within smoke-affected areas. Forest classes were identified with reliance on surrounding classes within non-smoke-affected areas. The smoked affected areas were classified using Spectral Angle Mapper classifier using the surface

reflectance from Landsat/ETM+ bands 4 (NIR), 5 (SWIR 1) and 7 (SWIR 2) which are less impacted by smoke. The reclassified sections were subsequently merged into the previous classification.

5.3 Post-classification processing

The developed classes from all steps of classification were combined into a single classification scheme according to legend presented in section 4. The resultant land cover map was sieved following the “>= 5 contiguous pixels” rule to eliminate speckle. The filtered pixels were assigned a max value from a 5X5 matrix. The matrix window was increased incrementally to 11X11 in cases where no distinct majority was identified at finer scales.

5.4 Accuracy assessment

Accuracy assessment was conducted following the accuracy assessment protocol developed by Dr. Krankina. It presents a combination of in situ data and randomly distributed additional points in classes that are poorly represented by ground data. The distribution of the accuracy assessment points overall proportional to the areal distribution of the mapped classes and consists of minimum of 300 randomly selected points across the image. For classes, where the proportional representation of 300 total points results in a sample of fewer than 30 points, additional random points are added to a minimum of 30 points in a sample class. According to the protocol two types of accuracy assessment are presented: 1) an assessment for 5 aggregated land cover classes including trees, shrubs, herbaceous cover, barren lands, and water; and 2) an assessment for the full set of classes identified within the site.

5.4.1 Aggregated classes accuracy assessment

For the accuracy assessment of the aggregated classes random points across the full extent of the classification were selected proportionally to the area of the class but no less than 30 pixels per class (see section 5.4). These random points were further assigned by the analyst to one of the 5 aggregated classes based on the surface reflectance characteristics and high resolution QuickBird images available at Google Earth.

		Observed Class					Sum	Commission
		Trees	Shrubs	Herbaceous	Barren	Water		
Predicted Class	Trees	215	3	0	0	0	218	1.38
	Shrubs	5	73	0	0	0	78	6.41
	Herbaceous	4	2	25	2	0	33	24.24
	Barren	0	3	5	28	0	36	22.22
	Water	1	0	0	0	30	31	3.33
	Sum	225	81	30	30	30	396	
Omission		4.44	9.88	16.67	6.67	0		
Overall Accuracy = 93.67								
Kappa Coefficient = 0.90								

5.4.2 Full classification accuracy assessment

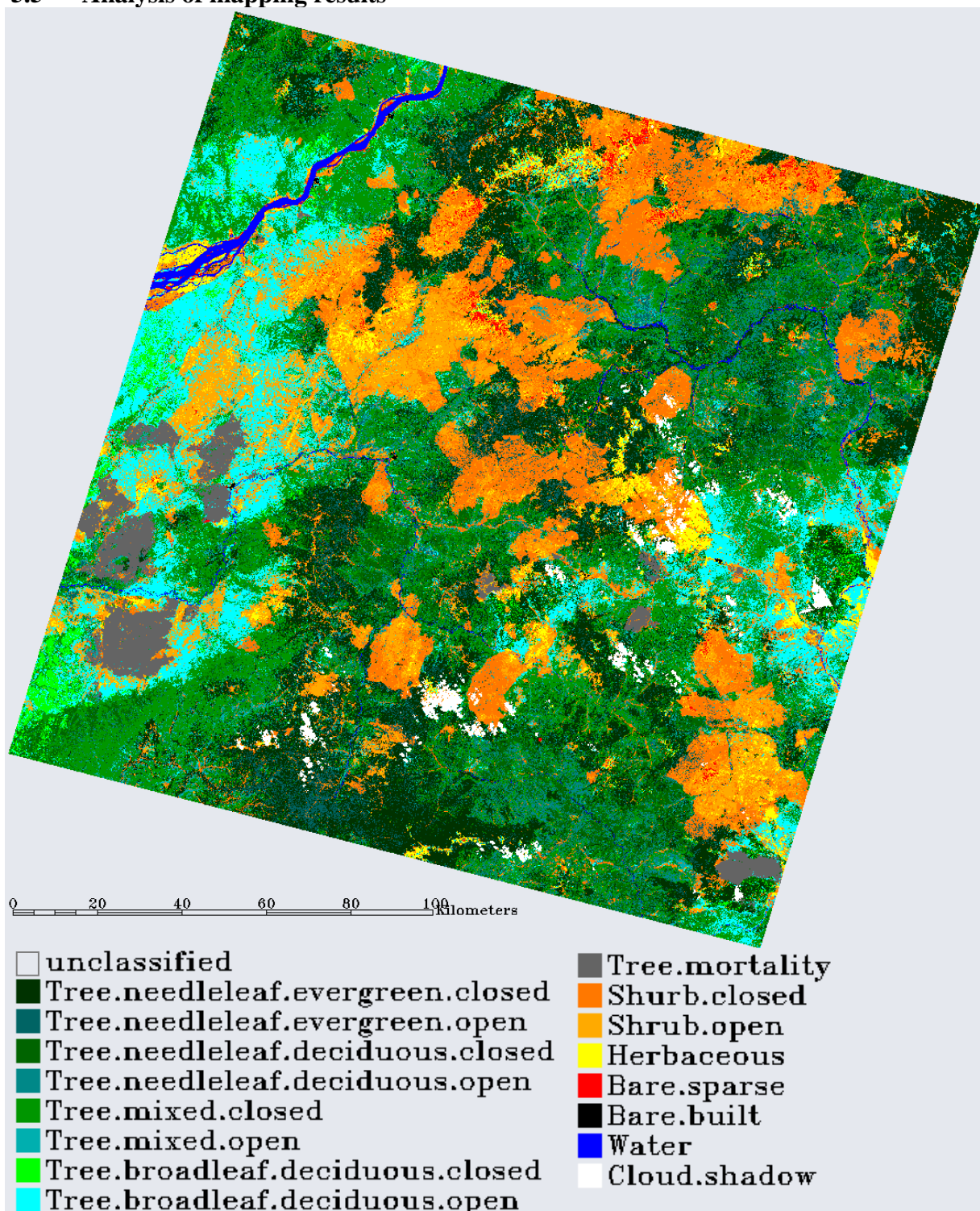
The full classification accuracy assessment was performed over a subset of the image where very high resolution imagery (e.g. Quickbird) was available in Google Earth. All classes had a representative sample within the high resolution validation data. The Herbaceous and Water class validation samples were adopted from the accuracy assessment for the aggregated classes. Selection of random points for the validation was limited to the extent of the available QuickBird imagery in Google Earth to ensure the ability to differentiate between classes. Random points which were not confidently identified by the analyst were removed from further validation and replaced with a new set of points. The most difficulty was encountered in differentiating Tree.needleleaved.deciduous classes in high or moderate resolution imagery therefore we expect a high range of uncertainty in mapping those classes.

Predicted Class	Observed Class															Sum	Commission (%)
	TNEC	TNEO	TNDC	TNDO	TMC	TMO	TBDC	TBDO	TM	SC	SO	H	BS	BB	W		
TNEC	52	4	0	0	1	0	0	0	0	0	0	0	0	0	0	57	8.77
TNEO	1	24	1	2	0	5	0	0	0	3	0	0	0	0	0	36	33.33
TNDC	0	0	24	0	6	0	0	0	0	0	0	0	0	0	0	30	20
TNDO	0	0	3	25	9	0	0	0	0	0	0	0	0	0	0	37	32.43
TMC	1	1	0	2	60	4	3	0	0	0	0	0	0	0	0	71	15.49
TMO	0	1	1	0	5	20	0	1	0	2	0	0	0	0	0	30	33.33
TBDC	0	0	0	0	0	0	30	0	0	0	0	0	0	0	0	30	0
TBDO	0	0	0	0	0	0	4	29	0	2	0	0	0	0	0	35	17.14
TM	0	0	0	0	0	0	0	0	29	1	0	0	0	0	0	30	3.33
SC	0	0	1	0	3	1	0	3	1	30	1	0	0	0	0	40	25
SO	0	0	0	0	0	0	0	1	0	2	32	0	0	0	0	35	8.57
H	0	0	0	0	0	0	0	0	0	0	0	25	0	0	0	25	0
BS	0	0	0	1	0	0	0	0	2	0	4	5	30	1	0	43	30.23
BB	0	0	0	0	0	0	0	0	0	0	1	0	0	29	0	30	3.33
W	0	0	0	0	0	0	0	0	0	0	0	0	0	0	29	29	0
Sum	54	30	30	30	84	30	37	34	32	40	38	30	30	30	29	558	
Omission (%)	3.7	20	20	16.7	29	33.3	18.9	14.71	9.4	25	16	17	0	3.3	0		

Overall Accuracy = 83.87%

Kappa Coefficient = 0.8258

5.5 Analysis of mapping results



The results of the Landsat/ETM+ classification were analyzed as percent of cover within the full extent of the Landsat scene (path 111 row 25). According to the classified image, closed mixed tree stands dominate the land cover of the Sikhote-Alin site (~21%). Overall tree dominated land

cover accounts for ~72% of the total area with the remaining area covered by shrubs (23%), herbaceous (2%), bare and sparse (1%) vegetation, and water (1%). Few human settlements are distributed along major roads with bare.built category accounting for 0.03% of the total scene.

Distribution of land cover classes

<i>Class</i>	<i>Pixel</i>	<i>Area (ha)</i>	<i>% of site</i>
Tree.needleleaf.evergreen.closed	7552297	613,435	18.04
Tree.needleleaf.evergreen.open	1928239	156,621	4.60
Tree.needleleaf.deciduous.closed	2773631	225,288	6.62
Tree.needleleaf.deciduous.open	1362861	110,698	3.25
Tree.mixed.closed	8806444	715,303	21.03
Tree.mixed.open	1770923	143,843	4.23
Tree.broadleaf.deciduous.closed	532964	43,290	1.27
Tree.broadleaf.deciduous.open	4427919	359,658	10.57
Tree.mortality	1048545	85,168	2.50
Shrub.closed	5255971	426,916	12.55
Shrub.open	4279487	347,601	10.22
Herbaceous	984409	79,959	2.35
Bare.sparse	293159	23,812	0.70
Bare.built	12843	1,043	0.03
Water	402920	32,727	0.96
Cloud.shadow	440764	35,801	1.05

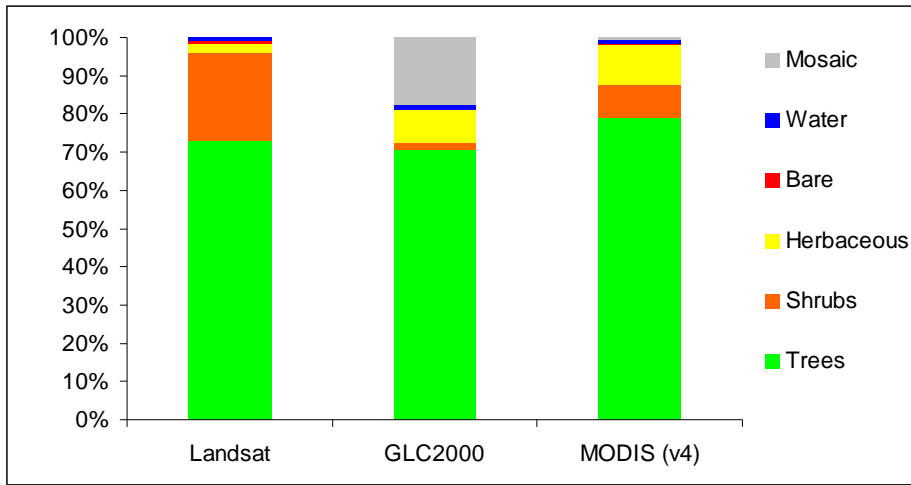
5.6 Comparison to coarse resolution land cover maps

The Landsat-based classification results were compared to the several coarse resolution products. Individual classes within each of the products were aggregated to general groups: tree dominates, shrub dominated, herbaceous dominated, bare, water and mosaic/other. IGBP-based classification was used for coarse resolution products. During the aggregation procedure cropland class was mapped as “herbaceous dominated”.

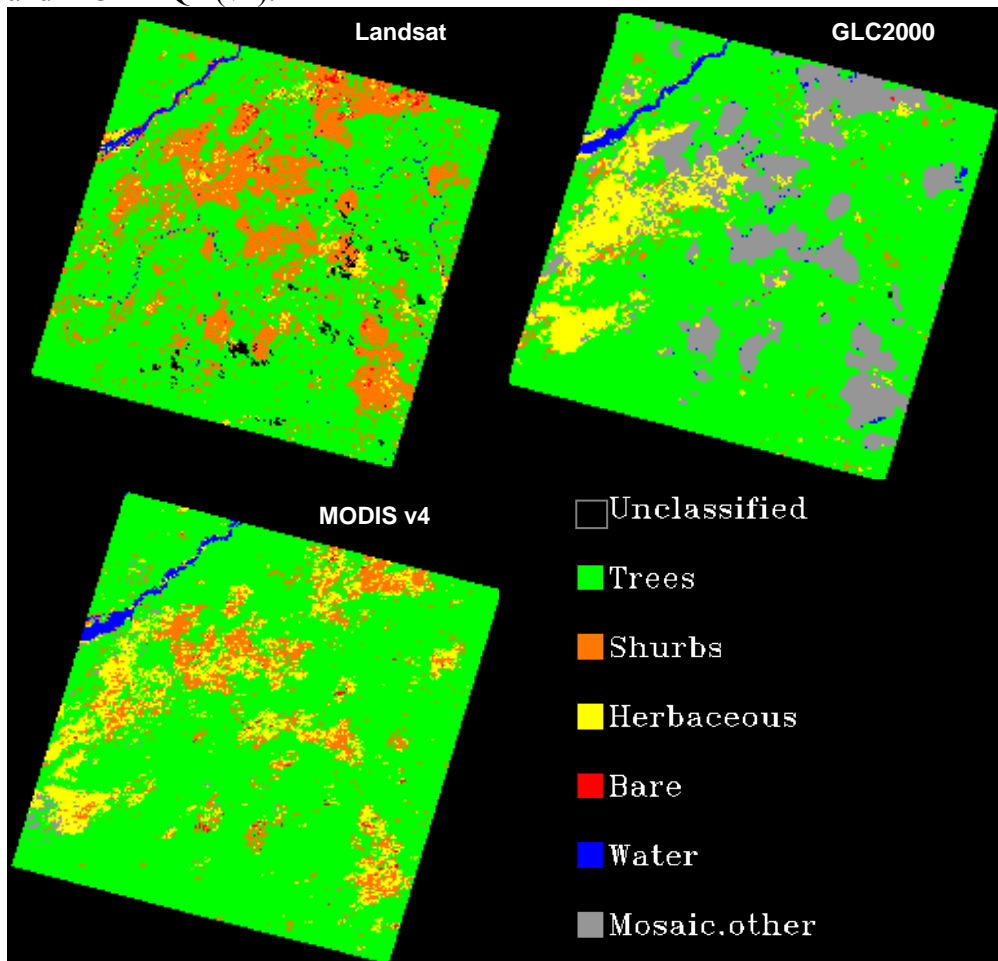
Distribution of aggregated land cover types in the Landsat, GLC2000, and MODIS (MOD12Q1) land cover products (percent):

<i>Class</i>	<i>Landsat</i>	<i>GLC2000</i>	<i>MODIS (v4)</i>
Tree dominated	72.131	70.815	78.955
Shrub dominated	22.772	1.719	8.718
Herbaceous dominated	2.351	8.564	10.482
Bare	0.731	0.052	0.265
Water	0.962	1.123	0.907
Mosaic and other	N/A	17.723	0.673

Percent land cover within the extent of the Landsat scene (path 111 row 25) mapped by the ETM+, GLC2000, and MOD12Q1 (v4).



Spatial variations in distribution of aggregated land cover types mapped by ETM+, GLC2000, and MOD12Q1 (v4).



6 Land Cover Change Map

6.1 Pre-processing

Three Landsat TM and ETM+ scenes for the study site were selected to use in change detection mapping: a) August 13, 1990, b) May 18, 2002; c) September 7, 2005 (see section 2). Each of the scenes was visually examined to determine its acquisition during the “leaf on” season and had minimal cloud cover. The scenes were geometrically co-registered to the scene from May 15, 2002 with RMS < 0.5. The scenes were converted to surface reflectance with correction of reflectance values according to variation in sun illumination angles due to topographic features using the methodology described in section 5.1.

6.1.1 Mature forest mapping

Water, shadow, cloud, and “mature forest” (defined by the analyst) were identified in the imagery. First, shadow, clouds, and water masks were created using band thresholding and subsequent analyst-driven selection. Second, multivariable stacks including surface reflectance for bands 1-5 and 7 and Tasseled Cap (TC) transforms (using surface reflectance coefficients (Crist, 1985)) for brightness, greenness, and wetness parameters were compiled for each scene. Third, maximum likelihood classification for four classes, including 1) bare and sparsely vegetated, 2) shrub dominated, 3) tree dominated, and 4) tree dominated with mortality classes with a 0.7 probability threshold was run on the 1990 and 2005 scenes masking out classes identified in step 1. Mature forests for 2002 image were identified based on the detailed classification including all tree dominated classes with the exception of “tree dominated with mortality” class.

6.1.2 Accuracy assessment for mature forest mapping

No sufficient in-situ data were available to provide accuracy assessment for the maximum likelihood classifications of mature tree category in 1990 and 2005 classifications. Subsequently the accuracy assessment is provided only based on the analyst’s visual interpretation of “mature tree” class vs “all other” classes following the overall assessment scheme described in section 5.4. According to this scheme, 300 random points were split between “mature trees” (>=150 points) and “all other” classes (>=150 points). The validation class assignment was done by the analyst’s on-screen interpretation of surface reflectance signatures in respective images. The results of accuracy assessments are provided below.

6.1.2.1 Scene from August 13, 1990

Accuracy assessment of mature tree class for 8/13/2005 shows that the maximum likelihood classification offers a reliable estimate of spatial distribution of mature tree class. The “mature tree” class has a higher omission error indicative of somewhat conservative estimate of tree dominated classes by the classification. Visual analysis confirms that the pixels classified as “other” and later identified by the analyst as “tree” are primarily found within areas with stronger soil signature characteristic for open communities.

		Observed Class			
		Trees	Other	Sum	Commission
Predicted Class	Trees	150	2	152	1.32
	Other	14	150	164	8.54
	Sum	164	152	316	
	Omission	8.54	1.32		
Overall Accuracy = 94.94%					
Kappa Coefficient = 0.90					

6.1.2.2 Scene from September 7, 2005

Accuracy assessment of mature tree class for 9/7/2005 shows that the maximum likelihood classification offers a reliable estimate of spatial distribution of mature tree class for this image as well.

		Observed Class			
		Trees	Other	Sum	Commission
Predicted Class	Trees	145	1	146	0.68
	Other	20	150	170	11.76
	Sum	165	151	316	
	Omission	12.12	0.66		
Overall Accuracy = 93.35%					
Kappa Coefficient = 0.8675					

6.2 Change detection

Change detection was based on the Disturbance Index (DI) methodology developed by Healy et al. (2005). The “mature forest” masks (section 6.1.1) were used to normalize the TC brightness, greenness, and wetness components to that of the mature forests following

$$B_r = (B - B_\mu) / B_\sigma$$

$$G_r = (G - G_\mu) / G_\sigma$$

$$W_r = (W - W_\mu) / W_\sigma$$

where B_r , G_r , W_r is rescaled Brightness, Greenness and Wetness, B_μ, G_μ, W_μ is mean Brightness, Greenness, and Wetness of “mature forest”, and $B_\sigma, G_\sigma, W_\sigma$ is standard deviation of Brightness, Greenness, and Wetness in “mature forest”.

The DI is then calculated following

$$DI = B_r - (G_r + W_r)$$

The common extent of the three scenes was defined and tree cover change was assessed using the maximum likelihood classification of the multi-temporal DI stack (1990-2002-2005). The training data was selected by the analyst based on visually identifiable disturbance and regrowth patterns within the three scenes. Forest change was mapped only within areas identified as “tree dominated” during any of the mapping years, i.e. 1990, 2002 or 2005. Areas with other dominant land cover types were masked out.

The three-time-steps change detection methodology allowed for identification of the following 8 classes of change.

Class	Class name	Description
1	dist_90_02	disturbance occurred between 1990 and 2002 with minimal subsequent regrowth by 2005
2	regr_90_02	regrowth between 1990 and 2002 with continuing regrowth by 2005
3	dist_02_05	disturbance occurred between 2002 and 2005
4	regr_02_05	regrowth between 2002 and 2005
5	dist_02_regr_05	disturbance occurred between 1990 and 2002 with noticeable subsequent regrowth by 2005
6	UF	unchanged forest
7	UNF	unchanged non-forest
8	fill	fill values including cloud cover, cloud shadows, and water

6.3 Post-classification processing

A 5-consecutive pixels minimum filter is run to eliminate potential noise of the resultant change. The eliminated pixels were filled using the iterative majority analysis within a 5X5 kernel. In cases where a 5X5 kernel was insufficient, the kernel size was increased sequentially to 7X7, 9X9, and 11X11.

6.4 Accuracy assessment

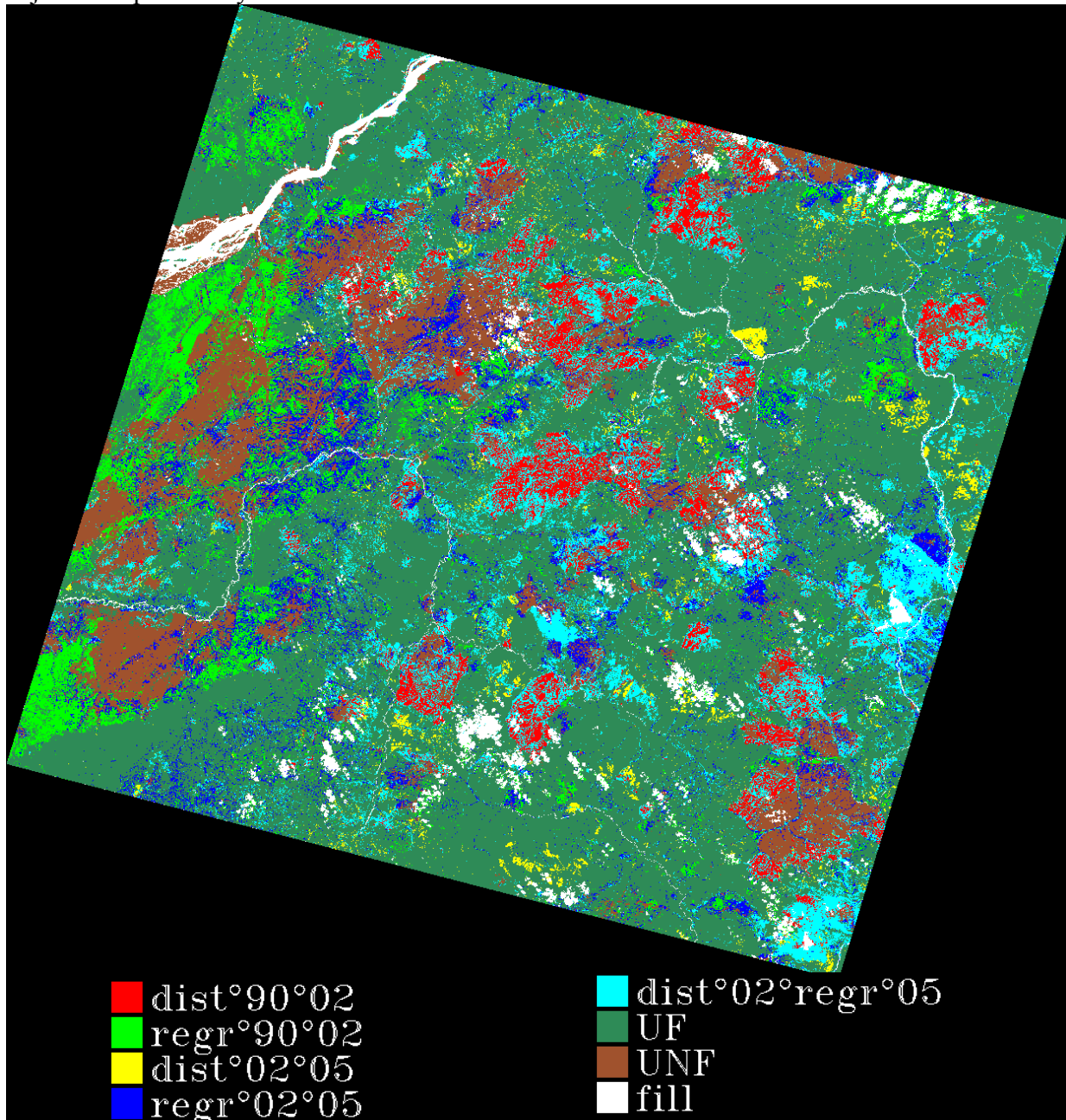
The accuracy assessment approach follows the random pixel selection and analyst interpretation described in section 5.4. The distribution of accuracy assessment points was split by ~150 pixels for “unchanged” and ~150 pixels for “changed” classes. Within each of the classes, the number of validation pixels was assigned proportionally to the class size but no less than 30 pixels.

		Observed class							Sum	Commission %
		UF	UNF	D_90_02	D_02_05	R_90_02	R_02_05	D02_R05		
Predicted class	UF	125	0	0	1	0	0	0	126	0.79
	UNF	0	28	0	0	0	10	3	41	31.71
	D_90_02	0	0	30	0	0	0	1	31	3.23
	D_02_05	0	1	0	27	0	0	0	28	3.57
	R_90_02	3	0	0	0	30	0	1	34	11.76
	R_02_05	10	1	0	0	2	24	4	41	41.46
	D_02_R05	8	2	8	2	0	1	43	64	32.81
	Sum	146	32	38	30	32	35	52	365	
Omission %	14.4	12.5	21.1	10	6.25	31.4	17.3			
Overall Accuracy = 84.11%										
Kappa Coefficient = 0.7996										

6.5 Results of the land cover change map

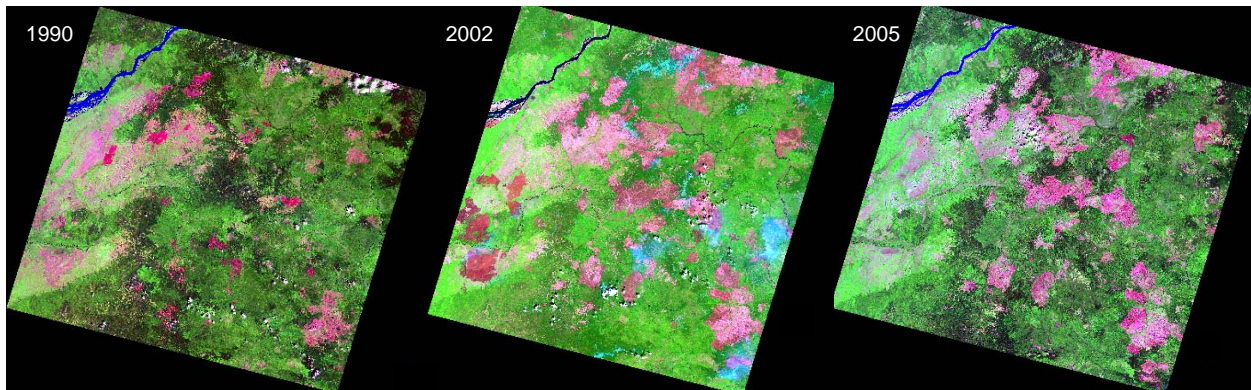
Between 1990 and 2005 the forests of the selected study site were altered by wildland fire occurrence, selective and clearcut logging activities and vegetation regrowth. Visual analysis

indicates that wildland fire is a significant recurring agent of forest disturbance and change. The landscape presents a mosaic of burn scars of various ages and at various forest growth stages across the entire scene. Visibly discernable fire scars are generally large and frequently are adjacent to previously burned areas.



The analysis indicates that more than 55% of forests in the study site remained undisturbed between 1990 and 2005. By 2005 nearly 30% of the site has undergone some type of conversion: from tree-dominated to other land cover types (6%), from non-tree dominated to tree-dominated land covers (13%), and from tree to non-tree-dominated landscapes and back to tree-dominated (10%). In this site restoration of tree dominated landscapes has surpassed conversion to non-tree-dominated landscapes. Tree growth occurs in this area at a considerable

rate with 10% of the scene under tree cover by 2005 when it was still visibly disturbed in early 2002. Visual analysis shows that faster rates of regrowth are found in logged sites and streambeds and flood planes within burn scars compared to those of burn scars on slopes or tops of hills and mountains. Approximately 12% of the study site has remained within non-tree dominated landscapes between 1990 and 2005 with the majority of the area found within previously burned sites. Visual analysis also indicates that some previously burned sites (particularly those in the left side of the image) have experienced repeated burning between 1990 and 2005.



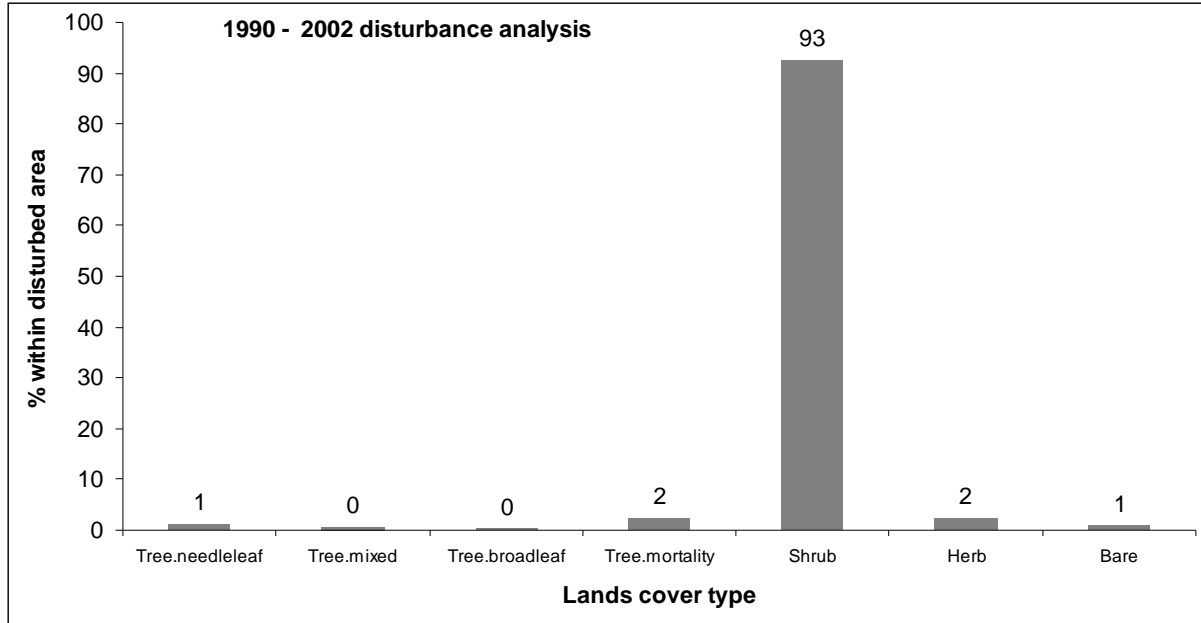
<i>Class</i>	<i>Pixels</i>	<i>Area (ha)</i>	<i>% study area</i>
dist_90_02	1832241	164901.7	5%
regr_90_02	2414054	217264.9	6%
dist_02_05	568720	51184.8	1%
regr_02_05	2660428	239438.5	7%
dist_02_regr_05	3957061	356135.5	10%
UF	21052644	1894738	55%
UNF	4531193	407807.4	12%
fill	1445146	130063.1	4%

6.6 Analysis of the land cover change map

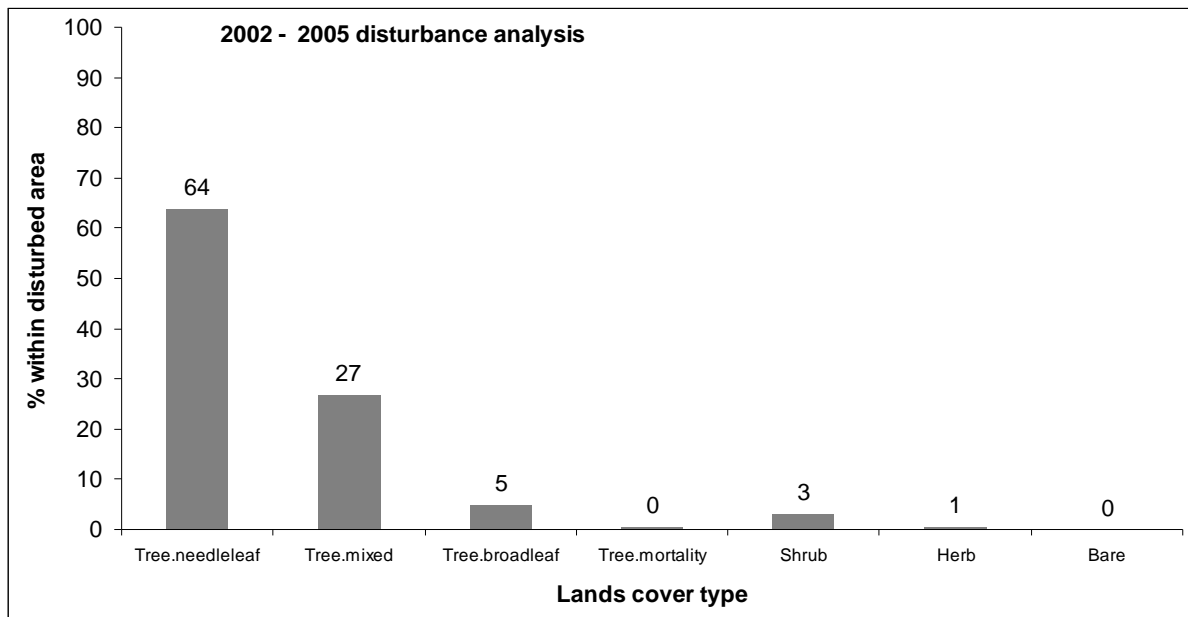
The analysis of the 1990-2002 disturbed areas in comparison with land cover distribution mapped from 2002 image shows that the absolute majority (93%) of disturbed areas were in a “shrub-dominated” stage of the community regrowth and did not return to tree-dominated communities. Recent fires resulted in development of tree-dominated with mortality landscapes on 2% of disturbed sites. Only 1% of disturbed areas returned to tree dominated communities by 2002 with 2% remaining in herbaceous land cover and 1% bare and sparsely vegetated landscapes.

The analysis of disturbances between 2002 and 2006 showed that 96% of affected areas were within tree dominated stands with ~64% within tree.needleleaf class, ~27% within tree.mixed class and ~5% within tree.broadleaf class. These findings are consistent with the previously published research which indicates that during large fire events needleleaf tree-dominated communities experience disproportionately larger amount of burning than other forest types (Loboda, 2009). The analysis of pre-2002 disturbances which demonstrated considerable amount of regrowth by 2005 shows that the majority (58%) of tree-dominated communities by 2005 developed from areas covered by mixed shrub dominated communities in 2002. Nearly 4%

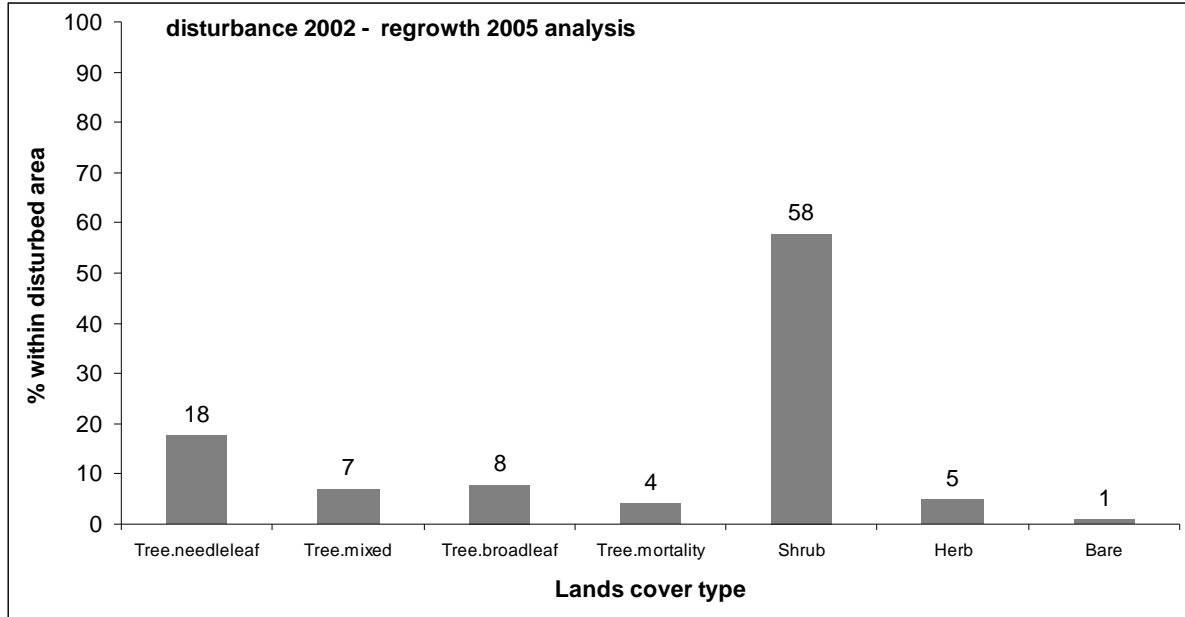
of areas with tree mortality in 2002 returned to tree-dominated communities by 2005. Those areas were primarily found in streambeds and flood planes as discussed in section 6.5. Over 33% of communities which were disturbed by 2002 were already in some stage of tree dominated land cover by 2002 which progressively got more closed by 2005.



Analysis of land covers (as mapped from 2002 image) within areas which were disturbed between 1990 and 2002. This figure indicates the stages of vegetation regrowth by 2002.



Analysis of land covers (as mapped from 2002 image) within areas which were disturbed between 2002 and 2005. This figure shows different rates of disturbance as a function of land cover type.



Analysis of land covers (as mapped from 2002 image) within areas which were disturbed by 2002 and converted to tree-dominated landscapes by 2005. This figure shows relative rates of vegetation recovery as a function of land cover type by 2005.

7 Publications Using the Site Data

None.

8 List of Contributors to Site Data and Report

Tatiana V. Loboda

University of Maryland
 Geography Department
 2181 LeFrak Hall
 College Park, MD 20742

Guoqing Sun

University of Maryland
 Geography Department
 2181 LeFrak Hall
 College Park, MD 20742

Zhiyu Zhang

University of Maryland
 Geography Department
 2181 LeFrak Hall
 College Park, MD 20742

9 Acknowledgements

This research was supported by the NASA Land Cover Land Use Change Program Grant # NS175AA.

10 References

- Chavez, P.S., Jr. (1996). Image-based atmospheric corrections: Revisited and improved. *Photogrammetric Engineering and Remote Sensing* **62**, 1025–1036.
- Crist, E.P. (1985). A TM Tasseled Cap Equivalent Transformation for Reflectance Factor Data. *Remote Sensing of Environment* **17**, 301-306.
- Healy, S.P., Cohen, W.B., Zhiqiang, Y., Krankina, O.N. (2005). Comparison of Tasseled Cap-based Landsat data structures for use in forest disturbance detection. *Remote Sensing of Environment* **97**, 301-310.
- Loboda, T. (2009). Modeling Fire Danger in Data-Poor Regions: A case study from the Russian Far East. **International Journal of Wildland Fire**, **18 (1)**: 19-35.
- Loboda, T., O’Neal, K.J., Csiszar, I. (2007). Regionally adaptable dNBR-based algorithm for burned area mapping from MODIS data. *Remote Sensing of Environment* **109**, 429-442.
- Soenen, S.A., Peddle, D.R., Coburn, C.A. (2005). SCS+C: A modified sun-canopy-sensor topographic correction in forested terrain. *IEEE Transactions on Geoscience and Remote Sensing* **43(9)**, 2148-2159.